Development of Shape Memory Alloy Actuated Gripper using Jamming Granular Effect

Miguel Santos Ramalho
miguelramalho@tecnico.ulisboa.pt

Instituto Superior Técnico, Universidade de Lisboa, Lisboa, Portugal

September 2020

Abstract

Most of robotic grippers implementations use rigid parts which have limitations. Soft robotics grippers are one of the solutions. Some of them are considered to be universal grippers as they are more versatile, grabbing almost any shape object (e.g. circular coins) and even fragile objects (e.g. eggs). However, a lot of these designs are dependent on air pressure which requires additional external and heavy pumps.

This study involves the design, construction and experimentation of a novel actuator mechanism for a soft-robotics universal gripper. The developed concept is based on a gripper that takes advantage of the granular jamming effect. It is similar as developed in [1], with the exception of incorporating a vacuum generation mechanism in a closed pneumatic circuit, making it independent from external devices. In order to produce this vacuum, a light actuation system uses a shape memory alloy (SMA) placed inside the gripper.

SMAs are light "smart" materials that have the ability to recover their original shape when exposed to an external factor like heat or magnetic field. SMAs have been previously used as actuator materials in soft robotics applications but usually not in the shape of a coiled spring, despite providing greater displacements.

To control the SMA spring, a system based on a microcontroller was developed.

The final SMA actuated universal gripper prototype is lightweight, compact and it was able to grip successfully objects with different shapes (sphere, coin, cube).

Keywords: Soft Robotics, SMA, Control, Spring, Jamming Granular Effect, Coil, Shape Memory Alloy

1. Introduction

Robotics' applications use discrete mechanisms, usually constructed from a series of rigid links. This is important for many industrial applications where the speed of operation and accuracy are essential. However, there are some limitations like weight/portability, safety concerns and speed. On different situations, other features may provide improved performance. To do so, scientists and researchers have recently turned to nature inspired robots (biomimetism or bio-inspired) [2]. Nowadays the field is known as soft robotics and these "new" found abilities have materialized in many diverse research fields [3].

However, the largest variety of devices and solutions in soft robotic research has been in grasping. With soft grippers it is possible to have more compliance, avoiding damaging shocks between the gripper and object. In this way, it also avoided damage to the desired path and position when manipulating the object. This combined with its simpler mechanic reduces control complexity. On the other hand, the soft grippers cannot house the actuators inside the links as it is done in rigid grippers, increasing the design complexity. The most commonly used materials in these grippers are elastomers, especially silicone rubbers [4].

Some of these soft grippers are considered universal grippers. The main advantage of an universal gripper is to save on precise positioning time when grasping a variety of objects with different shapes, and possibly random orientations. For this advantage to pay off, the operation time of the gripper should not exceed the positioning time of a conventional gripper. Some examples of soft grippers have already reached the market, albeit with different degrees of success. The best examples are the Flexshapegripper® (Festo corporate) and the Versaball® (Empire Robotics). Both of them are focused on the idea of a universal gripper, which

facilitates compliance, allowing to grip a wide variety of arbitrarily shaped object [5].
Some concerns are mentioned in [5] about designing and prototyping Versaball® prototype. The first is design modularity so that the gripper would be easy to replace (service life 1000 grips). The second concern was avoiding vacuum pumping systems that may not be available in most industrial facilities. In order to work around this problem, compressed air with a venturi pump was used. In [6], complex gripping problems like picking up flat objects (coins) and fragile objects (eggs) were overcome with this gripper. During this research work, some studies were done to understand the forces involved in keeping the object gripped to the membrane. The main variables in the gripper that affect the grasping capability are the membrane and the granular used inside the membrane.
The goal of this work is to show the feasibility of a self-contained soft gripper similar to the Versaball® griper described in [5]. Specifically, our version of the gripper contains its own means to produce the required vacuum, eliminating the need for an external vacuum source. This is done with a SMA actuator with only a small increase in the total weight of the gripper.

1.1. Shape Memory Alloys

Considerable research for modelling the microscopic and macroscopic behaviour of SMAs has been performed in the past fifty years [7].
The breakthrough for engineering applications occurred with the accidental discovery of a nickel-titanium alloy (NiTi-nitinol) by the US Naval Ordnance Laboratory (1961) while investigating materials useful for heat shielding [8, 9].
Since the release of the 1965 patent by the US Naval Ordnance Laboratory, the researched blossomed, mostly due to the properties of nitinol [8, 10–13]:

- Inexpensive to produce;
- high force to weight ratio;
- high wear and corrosion resistive;
- large reversible deformations (up to 8%);
- excellent structural and functional properties;
- easy and safer to handle than other SMAs;
- biocompatible and activated with body heat (no external power source);
- compatible with magnetic resonance imaging and computer tomography scanning;
- similarity to biological tissue mechanical response than conventional medical materials.

Despite all these advantages, SMAs require high currents. They are also difficult to control due to high non-linearity, hysteresis and constraints in frequency. These actuators have limited bandwidth. This means that no high frequencies should be used as they will give non-desirable results. This slow response is caused by the relatively high heat capacity of the metal [14, 15]. Also, thin SMA wires may pose challenges due to low electrical resistance [16].
Due to all SMA characteristics, many robotics implementations take advantages of these alloys abilities as actuators. Some of these systems include artificial muscles, origami robots microscopic grippers and robot prostheses (artificial limbs) [16, 17].
SMA actuators have various configurations and shapes, but the coil spring shape provides the largest stroke [18].
There have been different approaches to control the highly nonlinear behaviour of an SMA actuator. In [8] a review is made about exploring different control techniques. It is clear that the main concern is having a good model of the actuator behaviour. As the actuator is subject to variations that occur during the heat treatment, the development of actuator prototypes may require a case by case parameter identification.

2. Background

2.1. Universal Gripper

Jamming is the physical process that increases a material viscosity with the increase in density. This physical process is only visible on some mesoscopic materials, such as granular materials, glasses, foams, colloids, and other complex fluids.[19].
On one hand, the jammed state can resist small applied stresses without plastic deformation. This state is similar to a solid, with a characteristic maximum yield stress. On the other hand, the unjammed state allows flow with low resistance similar to a fluid [19].
This effect was applied in robotic grippers like [6]. In these grippers, the jamming granular material is closed inside a membrane. While the pressure value inside the membrane is similar to the outside pressure the gripper remains in the unjammed state. When the pressure inside the membrane is lower than the outside pressure, the granular material becomes jammed. This is shown in figure 1.

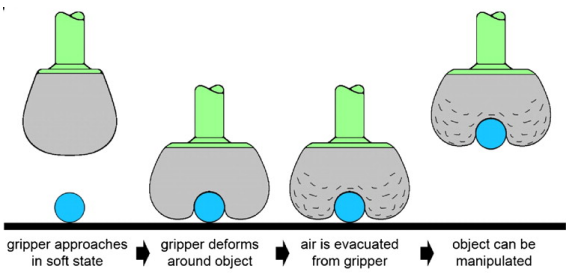

Figure 1: Schematic of a universal gripper gripping an object (from [1])

2.2. Shape Memory Alloys

SMAs can change between different phases called martensite, austenite. The martensitic phase is a state of the alloy noticeable by its low yield strength compared to its counterpart, the austenitic phase. Similarly, this phase is also characterized by lower shear and Young's modulus. So it is understandable why this phase will transform the same stress applied in a larger deformation of the material than the austenitic phase.

At lower temperatures, the fraction of the material with the martensitic phase is higher and the austenitic fraction phase is lower. In like manner, at higher temperatures, the opposite happens.

2.3. Shape Memory Alloy Springs

Helical springs are divided into three big groups, compression, extension and torsion springs. For the purpose of this gripper design, extension springs were chosen as the most suitable type. Compression springs are projected to resist compression forces [20].

When designing SMA springs some mathematical relations are relevant. First, the actuator has 3 working modes and lengths:

- The first is the phase which the actuator is not subject to any force and the material temperature is lower than the activation temperature ($T<T_{act}$), so it has all coils close together. The spring size in this working mode is identified as Li. Normally this is the spring in its state before being assembled into the system;
- The second is the spring subject to the maximum force and keeping the material in the martensitic phase (($T<T_{act}$)). This is the maximum length that spring will achieve and it is identified as Lm;
- The third is the spring subject to the maximum force and happens when the actuator has been active for a while ($T>T_{act}$). This is the length that spring will achieve when it is in its austenitic phase and it is identified as La.

Considering an ideal linear spring the Hooke's law can be applied with equation Castigliano's theorem:

$$\frac{F}{y} = k = \frac{d^4 G}{8D^3 N + 4DNd^2} \tag{1}$$

where F is the force in newtons, y is the spring displacement during an elongation without phase change (in m), k is called the spring constant, N is the number of active coils, F is the force in N, d is the wire diameter in m, G is the shear modulus in Pa, D is the mid diameter given by the outer diameter of the spring minus the wire diameter. The shear modulus is different for martensite and austenite thus this equation can only be applied to the same phase state of the SMA (austenitic or martensitic). where k is called the spring constant.

Considering only shear forces, the helicoidal spring elongation δ is related to the equivalent strain (Lagrangian) ϵ_{eq} at the external radius of the wire cross section ([8]):

$$\delta = Lm - Li = \frac{\pi N D^2}{d} \frac{\sqrt{3}}{2} \epsilon_{eq} \tag{2}$$

where δ is the spring displacement (not dependent on SMA phase state), ϵ_{eq} represents the equivalent strain.

3. Implementation

In order to find out the order of magnitude of the minimum pressure that would allow a reasonable grabbing, some tests were conducted. These tests also allowed to identify potential issues and better understand how this effect worked in practice.

For these preliminary tests, a version of the universal gripper was assembled. The minimum acceptable vacuum pressure found was 10^4 Pa.

3.1. Selection of Granular Material

The granular material must have three characteristics:

- High Yield strength during the jammed phase;
- Low friction resistance during the unjammed phase;
- Low density.

As there are many granular materials available, 5 different materials were chosen for comparison. All granular materials were chosen from [6] and [1], except for the expanded polystyrene that was chosen due to its low density. Also, different size grains of sodium chloride was used as a control because [5] mentions that grain size is one of the most critical properties in jamming performance.

Currently, no reliable mathematical models to simulate the yield strength of the jammed phase seem to be available in literature so it was necessary to devise a repeatable and reliable test to chose the right granular material for the gripper prototype. The solution was to perform some sort of a hardness test. As the Brinnel hardness test uses a sphere as an indenter, the results would be easily measured and less prone to errors. However using normalized sizes was not possible due to the small sphere diameter, so a manual hardness testing apparatus (figure 2) was designed and built. The sphere used in this apparatus had a diameter of 0,017 m.

The hardness tests were done using 2 different forces (5 and 10 N) and 2 different volume variations of the syringe (5 ml and 24 ml). The results of this hardness tests are presented in table 3 in the appendix. The hardness number was obtained using the equation (from [21]):

$$\mathrm{BHN} = \frac{2P}{\pi D(D - \sqrt{D^2 - d^2})} \tag{3}$$

where BHN is the Brinell Hardness Number, P is the applied load in kgf, D is the diameter of the indenter in mm, d is the diameter of the indentation in mm.

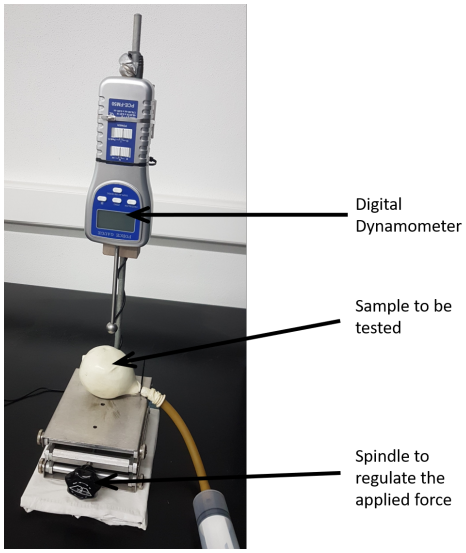

Figure 2: Picture of a Brinnel hardness test assembly

When comparing different grain sizes of sodium chloride, higher hardness values are obtained with smaller grain size as expected. The results were confirmed by what was seen when gripping objects with these materials at this stage. The only unexpected result was the low BHN of expanded polystyrene. This substance showed great results when picking up objects. This might be explained by the capability of the material to deform and better involve the grip object.
As for the low friction resistance during the unjammed phase, almost all of them proved to be fully reliable. The only granular material that had some problems was the milled coffee as it absorbed moist.
The density of each material is presented also in table 3. The tests to calculate the density were done with the granular materials at atmospheric pressure and at rest.
Based on these results the expanded polystyrene and coffee were chosen as the granular materials to be used in the design. These materials were both lightweight and had high gripping capacity.

3.2. Vacuum solutions

As the syringe size and diameter were fixed, there would not be enough freedom to adjust the dimensions and the force required to keep the desired pressure. So other solutions were attempted. The first solution was using industrial suction cups as a low friction device to generate vacuum. Despite the high diversity of this suction cups with detailed data sheets, these are not intended to be used extended when subject to negative pressure. Then using the concept of rolling lobe air (low-friction actuator[22]) a different idea emerged.
This idea was implemented according to the scheme in figure 3. On the left, the pressure inside the membrane (represented in green) is the atmospheric pressure, keeping the material in the unjammed state. The spring is not actuated and is fully extended. When the spring is contracted, the piston is pulled, increasing the volume and decreasing the pressure (material changes to jammed state).
To pull the piston back to the initial position, it is necessary another force, which was created by using rubber bands.

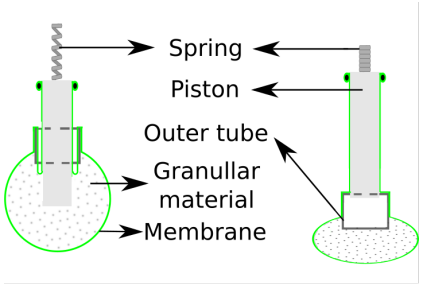

Figure 3: Schematic of the gripper developed

3.3. Design of Structural Elements

The next step of the design was to find a solution for clamping of the NiTi wire mentioned in [23]. This was done by placing each of the end coils of the spring between 2 flat copper plates as shown in picture 4.

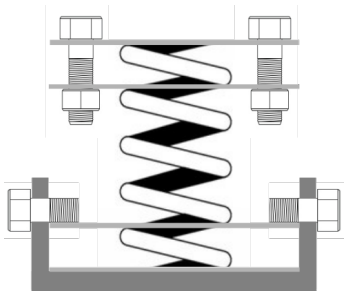

Figure 4: SMA clamping method applied. At each end of the spring, the last coil is pressured between two metal plates represented in gray lines.

In order to make sure that this prototype had the desired dimensions and a secure way of clamping the spring, it was mainly modelled in the software Solidworks® and later printed in a high density ABS 3D printer available at CENTI. A tensile

analysis was made to the most critical parts using finite elements. As the highest pressured using Von-Mises tensions (approximately 10^6 Pa) were much smaller than the Yield strength (approximately $3{\times}10^6$ Pa), no further analysis was needed. The next phase was ensuring that there was no air leakage so that the pressure inside the membrane remains stable. There were two techniques used to identify air leaks. The first consisted of submerging the gripper in water while increasing the pressure inside the membrane. The second technique was applying dish soap and water, which proved to be simpler and more efficient.

Obviously, the Fused Deposition Modeling technique used to print parts had micro holes that made the parts porous, letting air pass through. In order to correct this problem, two solutions were applied. First, the part was subject to a bath of hot acetone vapor ($(CH_3)_2CO$), this reacts with the external layers of the ABS parts resulting in a liquid mixture which fills some of the smaller holes. Secondly, ABS was coated with a layer of epoxy. To make sure no air would enter the system, a grove was made on the outside of the piston. The open end membrane was placed around this grove. Over the membrane, a higher diameter rubber ring was pressured using a zip tie. However, there were still visible air leaks so as a final solution the piston was replaced by manually machined nylon piece.

3.4. Fabrication of the Actuator

To develop a spring linear SMA actuator, it was required to shape the nitinol wire into a spring (cold-working) and then apply a heat treatment called annealing followed by quenching. The wire was acquired from the companies Nexmetal Corporation and Kellogg's Research Labs.

One of the most popular ways to give the wire the helicoidal shape is to wound it around a screw thread, with the same pitch as the wire's diameter. To achieve this a drilling machine, illustrated in figure 6, was used.

During the experiments, it was found that better results (less spaced coils) were obtained if the wire was wound in the counter-clockwise direction (Left hand-rule).This discovery opened new possibilities as every diameter size normalized threaded rod could produce springs with the minimum pitch using any diameter wire.

After testing several diameters wire it was found that wire with diameters bigger than $1{\times}10^{-3}$ m were too difficult to bend and would often break.

Figure 5 shows the apparatus during the training procedure and a spring before going into the furnace.

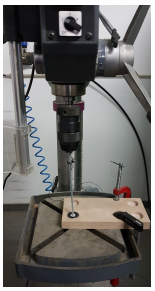

(a) Training procedure before turning on the driller

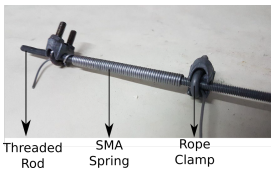

(b) Assembly with spring before heat treatment

Figure 5: SMA spring fabrication

3.5. Spring Design

In order to design an adequate spring, it was necessary to find the shear modulus (G). Consequently, tensile tests were made n (figure 6).

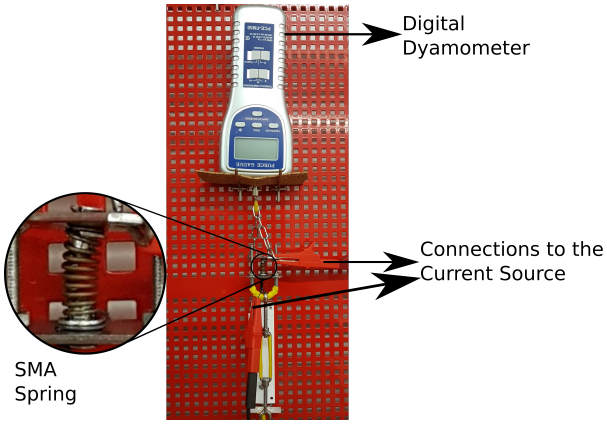

Figure 6: Tensile tests assembly

To perform these tests, different size springs were made. In this work, threaded rods with a nominal major diameter of $4{\times}10^{-3}$ m, $5{\times}10^{-3}$ m and $6{\times}10^{-3}$ m (M4, M5 and M6) were selected to produce springs with outer diameters of $5.7{\times}10^{-3}$ m, $6.7{\times}10^{-3}$ m and $7.7{\times}10^{-3}$ m, respectively. Then the springs were placed in the assembly of figure 6. With this assembly, values for spring elongation and applied force on the spring were collected. During this test, an infrared thermographic camera was used to ensure the spring was between 80 and 90 °C, avoiding too much functional fatigue while keeping the spring in the fully austenitic phase. It was noticeable during this tests that if the temperature was too high the spring would not fully recover its initial shape, whereas if the spring was stretched over the limit of functional fatigue no immediate decrease in shape recover was visible. The applied voltage was 1.1 V, being the current value 6.3 A. Approximating the values with a linear

function, the spring elastic constant (k) was found. From this value and using equation 1, the shear modulus for each spring was found. Using weighted arithmetic with the weights error (R^2) from each linear approximation, the value of 13.09×10^9 Pa was obtained which is the same order of magnitude than the values in [24].

As there are fewer constraints than the number of variables of a spring measurement it is difficult to find the best spring dimensions that prove the most effective for each application. With this in mind, it was necessary to develop a calculation design tool that uses generalized reduced gradient non-linear solving method to find the best result.

The variables were the diameter of the springs (limited to the threaded rods available) and the number of coils. The objective function to minimize was:

$$\begin{aligned} f(x) = w_1(\frac{\pi N D^2}{d}\frac{\sqrt{3}}{2}\epsilon_{eq} - y + La - Nd)^2 + \\ + w_2(F - \frac{d^4 G}{8D^3N + 4DNd^2}(La - Li))^2 + \\ + w_3(N - N_{rounded})^2 + w_4(D - D_{rounded})^2 + \\ + w_5 La + w_6\frac{La}{Li} \end{aligned} \quad (4)$$

Variables:

- D - spring diameter;
- d is the wire diameter in m;
- N - number of active coils.

Constraints:

- w_1 - weight of functional fatigue restriction (equation 2);
- w_2 - weight of the Castigliano's theorem (equation 1);
- w_3 - weight of the integer precision;
- w_5 - weight of the La size importance;
- w_6 - weight of the La size in respect to the Li importance;
- ϵ_{eq} - equivalent tensile strain;
- La - size of the spring when fully extended in martensitic phase (in m);
- F - force in N;
- G is the shear modulus in Pa;
- Li - size of the spring when fully compressed (in m).

Obtained from the solution:

- y - spring displacement during elongation in martensitic phase (in m);
- $N_{rounded}$ - number of active coils rounded to integers;
- $D_{rounded}$ - spring diameter rounded to integers.

For the weights the best values based on the speed of calculation and best results were found to be $w_1 = 0.8$, $w_2 = 0.9$, $w_3 = 1$, $w_4 = 100$, $w_5 = 1000$ and $w_5 = 0.5$. As constraints we admitted that the number of coils could only be bigger than 1, the size of coils could only be of a size that threaded rods could produce, La could only be bigger than Li, and that the first and second term of the objective function could not bigger than 0.09. The environment of this design tool can be seen in the picture 7.

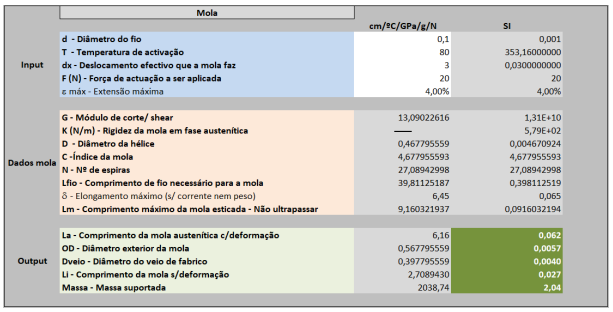

	Mola	cm/ºC/GPa/g/N	SI
Input	d - Diâmetro do fio	0,1	0,001
	T - Temperatura de activação	80	353,16000000
	dx - Deslocamento efectivo que a mola faz	3	0,0300000000
	F (N) - Força de actuação a ser aplicada	20	20
	ε máx - Extensão máxima	4,00%	4,00%
Dados mola	G - Módulo de corte/ shear	13,09022616	1,31E+10
	K (N/m) - Rigidez da mola em fase austenítica	—	5,79E+02
	D - Diâmetro da hélice	0,467795559	0,004670924
	C -Índice da mola	4,677955593	4,677955593
	N - Nº de espiras	27,08942998	27,08942998
	Lfio - Comprimento de fio necessário para a mola	39,81125187	0,398112519
	δ - Elongamento máximo (s/ corrente nem peso)	6,45	0,065
	Lm - Comprimento máximo da mola esticada - Não ultrapassar	9,160321937	0,0916032194
Output	La - Comprimento da mola austenítica c/deformação	6,16	0,062
	OD - Diâmetro exterior da mola	0,567795559	0,0057
	Dveio - Diâmetro do veio de fabrico	0,397795559	0,0040
	Li - Comprimento da mola s/deformação	2,7089430	0,027
	Massa - Massa suportada	2038,74	2,04

Figure 7: Spring design tool environment

3.6. Sensors and Control

To control and study the behaviour of this prototype, some sensors needed to be implemented (pressure, current and temperature sensors). The SMA spring is actuated with a n-channel MOSFET by PWM signal. The control, analogue reading, analogue to digital conversion is made using an Arduino® Uno. A schematic of all the connections is shown in figure 8.

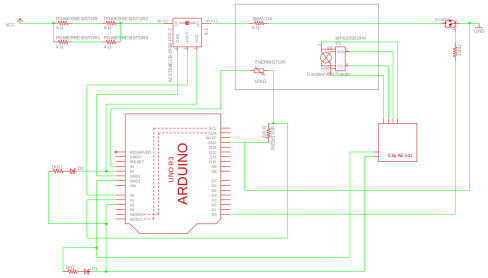

Figure 8: Schematic of the electrical connections

A control of the type on-off was implemented. The spring was heated until the temperature was 75°C as this would avoid an overshoot over the 80 °C affecting the functional fatigue. After this, the current would only be turned on if the spring temperature would lower bellow 60 °C.

4. Experiments

4.1. Cycle Analysis

There was a need to test if the prototype did work similar to [1, 5, 6, 25] and also find its limitations. The first step to obtain these answers was to collect the sensor data during a full activation and relaxation of the actuator without using the gripper to grip any object (figure 9).

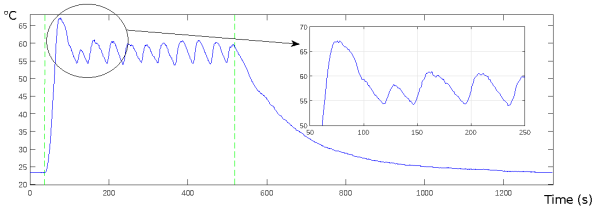

(a) Readings from the temperature sensor in °C along the time in s

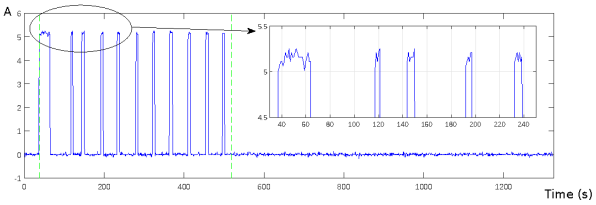

(b) Readings from the current flow sensor in A along the time in s

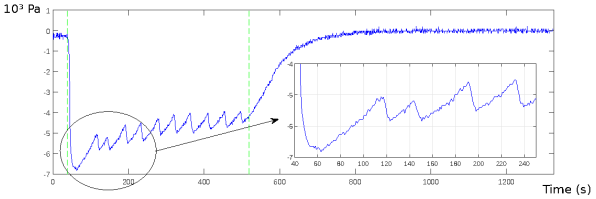

(c) Readings from the pressure sensor in 10^3 Pa along the time in s

Figure 9: Readings from the temperature sensor (top), current flow sensor (middle) and pressure sensor (bottom) during a full actuation and de-actuation cycle. The x-axis is time and the y-axis is temperature, current and pressure, respectively. The first green dashed line represents the moment when the gripper was activated and the second is the time it was turned off.

There is an overshoot of the temperature, 15% reaching 67 °C after 38 s of the initial activation period to heat the SMA. This period is 29 s long. The next activation period is only given after 51 s when the temperature is below 55 s. The next activation does not last longer than 5 s keeping the temperature between 54 and 61 °C, which is enough to keep the SMA with a low martensitic fraction (ξ). This value of ξ is enough to maintain a vacuum pressure suitable for gripping objects.

It takes more time to lower its temperature than to increase it, which is expected since this is a thermal system using only natural convection. As for the pressure, it took a similar amount of time to reach the desired pressure as to reach the desired temperature (26 s) but took a lot lesser time than the temperature to recover the original value (297 s). This might be explained by the loss of vacuum due to small leaks.

However, the relation between the temperature and the pressure is visible. As the temperature rises, the pressure lowers and vice versa. So a transformation function, that scales and moves the pressure across the vertical axis can be found so this similarity can be studied. This transformation is shown in figure 10 (a). In this figure it is noticeable across all the response, turning on the current produces an immediate effect on the pressure sensor readings, which shows that the Joule effect is an effective way of actuating an SMA spring.

Another representation of the data is shown in figure 10(b), instead of showing the evolution across time this graphic shows the pressure in function of the temperature. It is visible a series of circles between 54 and 63 °C and between -3.5×10^3 and -6×10^3 Pa. These circles are caused by the control turning on and off the actuator, changing the martensitic fraction. This is not a single cycle because there are the pressures losses, sliding each circle as the negative pressure is lost. It is noticeable that activating the gripper to grip a part is a lot faster than recovering its original pressure to be able to grip another part.

In this test, it became clear that the system worked and could create the minimum pressure to grab an object during a reasonable amount of time. Also, this type of control proved to be effective in maintaining a pressure value.

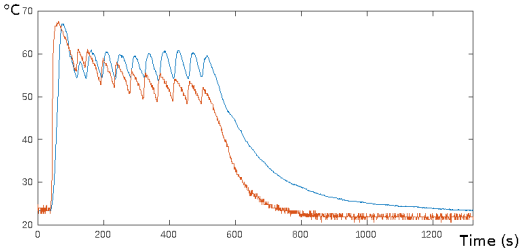

(a) Readings from the current pressure sensor in red and adjusted readings from the pressure sensor in blue along the time in s

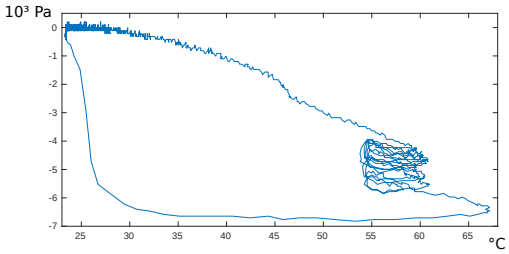

(b) Evolution of pressure (the vertical axis) with the temperature (horizontal axis)

Figure 10: In the top graphic is presented the readings from the temperature sensor as blue line along with adjusted pressure sensor readings as a red line. The bottom graphic represents the change in pressure as the temperature changes.

4.2. Gripping Tests

The next tests consisted of doing grip success tests. In order to do this test, there was the need to chose different objects. So 4 different shapes were chosen based on [1] Euro coins and PLA (Poly Lactic Acid) 3D printed objects were used. The sizes chosen were 50% and 75% of the gripper size (approximately 4×10^{-2} m), to respect the adequate sizes mentioned in [5]. The weights and a picture of these 8 objects are shown in table 1 and figure 11, respectively.

Originally, the test consisted of grabbing the object 7 times and checking whether the object stayed gripped during at least 20 s. However, after verifying that the results were always the same, it was chosen to do only 1 grip test for each object, using 3 different granular materials: small sphere of polystyrene (3×10^{3} m diameter), couscous (2×10^{3} m diameter) and milled coffee. A total of 24 experiments were done.

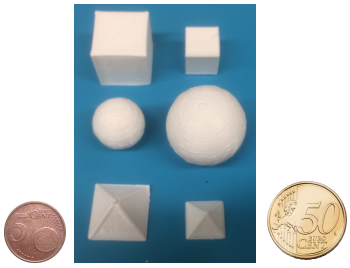

Figure 11: Objects used for gripping tests

Table 1: Gripping tests Pieces

Object	Weight (g)	
	50% gripper size	75% gripper size
sphere	1.82	4.92
cube	4.15	1.65
pyramid	1.48	0.61
5 cent coin	3.92	
50 cent coin	7.80	

These experiments were done by filling the membrane with 30 ml of granular material (polystyrene for the first tests) which presented low gripping capabilities. So after some testing, the filling was changed to 50 ml of granular material and this time the success rate was always the same as presented in table 2.

As stated in table 2 the only parts that the gripper could not grab with success where the pyramids and the 50 cent coin. This is in accordance with the holding force measured in [1].

There were experiments where the initial pressure was not zero, some of these experiments did not reach pressures lower than -5×10^{3} Pa. These experiments were not considered in the final results, but nevertheless showed an interesting fact. Despite the smaller vacuum the gripper could still be used to grip successfully the smallest objects (50% of the gripper size).

The polystyrene seemed to grip the part better because even in the case of misalignment the part was grabbed as in the other fillers they would mostly fall out. Also, it was the only granular material that was able to lift the 50 cent coin from the surface despite not holding for the 20 s stated. The pyramids could only be gripped if the base edge was facing upwards instead of the top.

Table 2: Success rate on 7 trial experiment with 50 ml polystyrene as filler material

Object	Successful grip	
	50% gripper size	75% gripper size
sphere	7/7	7/7
cube	7/7	7/7
pyramid	0/7	0/7
5 cent coin	7/7	
50 cent coin	0/7	

The first fact that must be reported is the similarity of these tests results (figure 12) to the one shown in figure 9. One difference is the moment the gripper touches the part, producing a slight increase in pressure (cyan circle). The second difference is the moment that the piece is lifted from the plane (green circle), producing a slight increase in pressure. In some cases, this smaller difference is not visible due to the sensor noise. As for the moment the object falls off the gripper, no change is visible in any of the sensors values.

As explained in [1], positive pressure after a grip is important to get a better grip on the next object so a full recovery of the initial pressure is needed.

One of the difficulties of this experiment is the force done while pushing the gripper against the object. As the granular material might not be exactly in the same position the force applied has to be regulated by the increase in pressure.

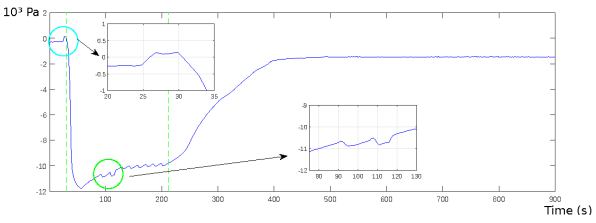

Figure 12: Readings from the pressure sensor. The 50% sized sphere was grabbed using polystyrene as grip filler.

5. Conclusions

It was demonstrated that a variable volume closed system is a viable approach to generate the vacuum pressure required to drive a granular jamming gripper. So the main objective of this work was achieved.

A new method (hardness tests) to select granular materials was also proposed. This experiment along with the experiments of gripping objects shows that a certain degree of deformability may be desirable to optimize the application of jamming granular effect to gripping objects. This was demonstrated when expanded polystyrene did show the most flexibility with gripper and test object misalignment, despite having a smaller BHN than milled coffee used in [5]. It also made the gripper lighter and avoided the humidity sensibility present in coffee.

After several attempts, the method of producing spring was perfected so that tightly springs without spacing between coils were obtained. So there is a reasonable degree of certainty in the fact that this method of producing springs is a good alternative to the lathe machine.

As for the last experiments, it was proven that a PWM actuation with an on-off control is efficient in this application and did not produce any detectable functional fatigue of the actuator. The sensor system was able to provide the necessary data pressure and temperature to show that the system is very fast to activate but slow to recover to its initial condition. The recorded time to full recovery of the original pressure value was close to 600 s, which is not acceptable for a practical application of the device, but more can be done to improve recovery time.

In the analysis of the experiment, it was found a relation between the temperature and pressure and it was observed that the actuator was working in a safe zone where the martensite fraction was not zero.

Finally, the gripping tests demonstrated that a self-contained actuator is a viable answer to solve issues such as weight, noise, compactness and additional compressors or electric motors.

Acknowledgements

First of all, I would like to thank all my thesis supervisors for their availability and counseling. Secondly I would like to thank both IST and CENTI for both the materials and laboratories that allowed to develop this work.

References

[1] Eric Browna, Nicholas Rodenberga, Hod Lipsonb , John Amendb , Annan Mozeikac , Erik Steltzc , Mitchell R. Zakind, Jaegera, and Heinrich M. Universal robotic gripper based on the jamming of granular material. *IEEE Transactions on Robotics*, 28(2):341–350, 2010.

[2] J.B.C. Davies G. Robinson. Continuum Robots - A State of the Art. *Conference on Robotics and Automation*, (May):2849–2854, 1999.

[3] Cecilia Laschi, Barbara Mazzolai, and Matteo Cianchetti. Soft robotics: Technologies and systems pushing the boundaries of robot abilities. *Science Robotics*, 1(1):eaah3690, 2016.

[4] Jun Shintake, Vito Cacucciolo, Dario Floreano, and Herbert Shea. Soft Robotic Grippers. *Advanced Materials*, 1707035(May), 2018.

[5] John Amend, Nadia Cheng, Sami Fakhouri, and Bill Culley. Soft Robotics Commercialization: Jamming Grippers from Research to Product. *Soft Robotics*, 3(4):213–222, 2016.

[6] John R. Amend, Eric Brown, Nicholas Rodenberg, Heinrich M. Jaeger, and Hod Lipson. A positive pressure universal gripper based on the jamming of granular material. *IEEE Transactions on Robotics*, 28(2):341–350, 2012.

[7] Mohammad H. Elahinia and Hashem Ashrafiuon. Nonlinear Control of a Shape Memory Alloy Actuated Manipulator. *Journal of Vibration and Acoustics*, 124(4):566, 2002.

[8] Mohammad Elahinia. *Shape Memory Alloy Actuators: Design, Fabrication and Experimental Evaluation*. 2016.

[9] P K Kumar and D C Lagoudas. Shape Memory Alloys. 1, 2008.

[10] Ferdinando Auricchio, Elisa Boatti, and Michele Conti. *SMA Biomedical Applications*. Elsevier Ltd, 2014.

[11] Donald J L Leo. *Engineering Analysis of Smart Material Systems*. 2007.

[12] Jaronie Mohd Jani, Martin Leary, and Aleksandar Subic. Shape Memory Alloys in Automotive Applications. *Applied Mechanics and Materials*, 663:248–253, 2014.

[13] K. Ikuta. Micro/miniature shape memory alloy actuator. *Proceedings., IEEE International Conference on Robotics and Automation*, pages 2156–2161, 1990.

[14] D. J. Hartl and D. C. Lagoudas. Aerospace applications of shape memory alloys. *Proceedings of the Institution of Mechanical Engineers, Part G: Journal of Aerospace Engineering*, 221(4):535–552, 2007.

[15] A. Hadi, A. Yousefi-Koma, M. Elahinia, M. M. Moghaddam, and A. Ghazavi. A shape memory alloy spring-based actuator with stiffness and position controllability. *Proceedings of the Institution of Mechanical Engineers. Part I: Journal of Systems and Control Engineering*, 225(7):902–917, 2011.

[16] Mohammad Mahdi Kheirikhah, Samaneh Rabiee, and Mohammad Ehsan Edalat. A Review of Shape Memory Alloy Actuators in Robotics. pages 206–217, 2011.

[17] Barry a Trimmer, Ann E Takesian, Brian M Sweet, Chris B Rogers, Daniel C Hake, and Daniel J Rogers. Caterpillar locomotion : A new model for soft- bodied climbing and burrowing robots. *7th International Symposium on Technology and the Mine Problem, Monterey, CA May 2-5, 2006*, (April 2002):1–10, 2006.

[18] T. Ishii. *Design of shape memory alloy (SMA) coil springs for actuator applications*. Woodhead Publishing Limited, 2011.

[19] Dapeng Bi, Jie Zhang, Bulbul Chakraborty, and R. P. Behringer. Jamming by shear. *Nature*, 480(7377):355–358, 2011.

[20] R. Budynas and K. Nisbett. *Shigley's Mechanical Engineering Design*. McGraw-Hill Education, 2010.

[21] J. P. Davim and A G. Magalhães. *Ensaios Mecânicos e Tecnológicos*. Publindústria, 2010.

[22] Ilnterautomatika datasheets. `http://interautomatika.lt/download/Diaphragm%20Air%20Cylinders%20datasheet_ENG.pdf`. Accessed: 2020-04-10.

[23] Jaronie Mohd Jani, Martin Leary, Aleksandar Subic, and Mark A. Gibson. A review of shape memory alloy research, applications and opportunities. *Materials and Design*, 56:1078–1113, 2014.

[24] Globalspec database. `http://www.matweb.com/search/datasheettext.aspx?matguid=44afc7d3c6eb4829bc2df27884fd2d6c`. Accessed: 2020-07-10.

[25] E. Brown, N. Rodenberg, J. Amend, a. Mozeika, E. Steltz, M. R. Zakin, H. Lipson, and H. M. Jaeger. From the Cover: Universal robotic gripper based on the jamming of granular material. *Proceedings of the National Academy of Sciences*, 107(44):18809–18814, 2010.

6. Appendix

Table 3: Brinnel test

Granular Material		Sodium Chloride				Expanded polystyrene		Milled Coffee		Sand	
		Fine Grains		Coarse Grains							
Volume (m^3)		7×10^{-5}									
Mass (g)		113.74		126.4		16.79		40.06		126.4	
Density (10^3 Kg/m^3)		1.62		1.81		0.24		0.57		1.81	
Volume variation 5ml	Force (N)	10	25	10	25	10	25	10	25	10	25
	indentation (10^{-3} m)	10	13	12	16	22	25	9	10	6	9
	BHN (10^6 Pa)	0.122	0.175	0.083	0.109	0.019	0.025	0.151	0.305	0.348	0.379
Volume variation 24 ml	Force (N)	10	25	10	25	10	25	10	25	10	30
	indentation (10^{-3} m)	7	9.5	10	14	14	16	6	10	5	7.5
	BHN (10^6 Pa)	0.254	0.301	0.122	0.148	0.059	0.109	0.348	0.305	0.504	0.663